



This is a repository copy of *TREX exposes the RNA-binding domain of Nxf1 to enable mRNA export.*

White Rose Research Online URL for this paper:  
<http://eprints.whiterose.ac.uk/101507/>

Version: Accepted Version

---

**Article:**

Viphakone, N., Hautbergue, G.M. [orcid.org/0000-0002-1621-261X](https://orcid.org/0000-0002-1621-261X), Walsh, M. et al. (5 more authors) (2012) TREX exposes the RNA-binding domain of Nxf1 to enable mRNA export. *Nature Communications*, 3. 1006. ISSN 2041-1723

<https://doi.org/10.1038/ncomms2005>

---

**Reuse**

Unless indicated otherwise, fulltext items are protected by copyright with all rights reserved. The copyright exception in section 29 of the Copyright, Designs and Patents Act 1988 allows the making of a single copy solely for the purpose of non-commercial research or private study within the limits of fair dealing. The publisher or other rights-holder may allow further reproduction and re-use of this version - refer to the White Rose Research Online record for this item. Where records identify the publisher as the copyright holder, users can verify any specific terms of use on the publisher's website.

**Takedown**

If you consider content in White Rose Research Online to be in breach of UK law, please notify us by emailing [eprints@whiterose.ac.uk](mailto:eprints@whiterose.ac.uk) including the URL of the record and the reason for the withdrawal request.



[eprints@whiterose.ac.uk](mailto:eprints@whiterose.ac.uk)  
<https://eprints.whiterose.ac.uk/>

Published in final edited form as:

*Nat Commun.* 2012 ; 3: 1006. doi:10.1038/ncomms2005.

## TREX exposes the RNA binding domain of Nxf1 to enable mRNA export

Nicolas Viphakone<sup>1</sup>, Guillaume M. Hautbergue<sup>1</sup>, Matthew Walsh<sup>1</sup>, Chung-Te Chang<sup>1</sup>, Arthur Holland<sup>1</sup>, Eric G. Folco<sup>2</sup>, Robin Reed<sup>2</sup>, and Stuart A. Wilson<sup>1,\*</sup>

<sup>1</sup>Department of Molecular Biology and Biotechnology, The University of Sheffield, Firth Court, Western Bank, Sheffield, S10 2TN, U.K.

<sup>2</sup>Department of Cell Biology, Harvard Medical School, 240 Longwood Avenue, Boston, Massachusetts 02115, USA.

### Abstract

The metazoan TREX complex is recruited to mRNA during nuclear RNA processing and functions in exporting mRNA to the cytoplasm. Nxf1 is an mRNA export receptor, which binds processed mRNA and transports it through the nuclear pore complex. At present, the relationship between TREX and Nxf1 is not understood. Here we show that Nxf1 uses an intramolecular interaction to inhibit its own RNA binding activity. When the TREX subunits Aly and Thoc5 make contact with Nxf1, Nxf1 is driven into an open conformation, exposing its RNA binding domain, allowing RNA binding. Moreover, the combined knockdown of Aly and Thoc5 drastically reduces the amount of Nxf1 bound to mRNA *in vivo* and also causes a severe mRNA export block. Together, our data indicate that TREX provides a license for mRNA export by driving Nxf1 into a conformation capable of binding mRNA.

The Nxf1 protein (also known as Tap in humans and Mex67p in yeast<sup>1,2,3,4</sup>, Fig. 1a), functions as an export receptor for mRNA. Human Nxf1 (hereafter referred to as Nxf1) binds RNA through an N-terminal arginine-rich RNA binding domain (RBD) and this activity is essential for mRNA export<sup>5,6</sup>. Multiple arginines within the Nxf1 RBD are required for interaction with RNA *in vitro* and with poly(A)<sup>+</sup> RNA *in vivo*, and thus may provide a charged platform for RNA interactions<sup>6</sup>. The Nxf1 RBD displays no obvious sequence specificity and binds a variety of RNA substrates<sup>5,6</sup>. Once bound to mRNA, Nxf1 escorts the messenger ribonucleoprotein (mRNP) to the nuclear pore, where Nxf1 interacts with nucleoporins via the NTF2-like (NTF2L) and UBA domains<sup>7</sup>. Normally, mRNA is only exported to the cytoplasm upon completion of mRNA processing, though how the cell orchestrates the timely export of mRNA through the Nxf1 pathway is not clear.

The TREX complex<sup>8</sup> plays an important but undefined molecular function in mRNA export. TREX comprises a core THO complex which consists of Thoc2, Hpr1, Thoc5, Thoc6, Thoc7 and Tex1 in metazoans<sup>9,10</sup> and Tho2p, Hpr1p, Mft1p and Thp2p in yeast<sup>11</sup>. The human THO complex assembles in an ATP-dependent manner with the RNA helicase Uap56, Aly and Cip29<sup>12</sup>. The TREX complex is recruited to spliced mRNA<sup>10</sup> near the 5' cap<sup>13</sup>. Furthermore, Yra1, the yeast orthologue of Aly is delivered to the TREX complex during 3' end processing by Pcf11, and the Pcf11-Aly interaction is conserved in humans<sup>14</sup>.

\*To whom correspondence should be addressed: stuart.wilson@sheffield.ac.uk.

**Authors contributions** N.V., R.R. and S.W. designed experiments. N.V., G.H., M.W., C.C., A.H. and E.F. performed the experiments. N.V., R.R. and S.W. wrote the manuscript.

**Competing financial Interests statement** The authors declare that they have no competing financial interests.

Two TREX components, Aly and Thoc5, bind directly to Nxf1. Aly associates with the N-terminal RBD and adjacent  $\psi$ RRM of Nxf1 (Fig. 1a)<sup>15</sup> and this interaction is conserved in yeast<sup>16</sup>. Aly binds RNA via an arginine-rich peptide<sup>17</sup> which doubles as the binding site for Nxf1. When Nxf1 is recruited to an Aly:RNA complex, the RNA is handed over from Aly to Nxf1, and Aly enhances the RNA binding activity of Nxf1 by an undefined mechanism<sup>6</sup>. The NTF2-like (NTF2L) domain of Nxf1 (Fig. 1a) binds Thoc5 *in vitro*, and Thoc5 and Aly bind simultaneously to Nxf1 *in vitro*, though the functional consequences of Thoc5 binding are not clear<sup>18</sup>. Finally, in yeast, Hpr1 associates with the C-terminal UBA domain of Mex67, which is conserved in Nxf1. This interaction is enhanced by Hpr1 ubiquitinylation and drives recruitment of Mex67 to sites of transcription<sup>19</sup>. Nxf1 and TREX exist on the same mRNA<sup>18</sup>, though these interactions may be bridged by mRNA, and it is not clear whether Nxf1 associates via protein-protein interactions with assembled TREX *in vivo*. In yeast, loss of TREX components triggers a rapid mRNA export block<sup>8</sup> though RNAi of most metazoan TREX components results in a less striking mRNA export block<sup>18,20</sup>. The protein Uif, whose abundance increases significantly following Aly RNAi, compensates for Aly knockdown<sup>20</sup>. Consistent with these data, double knockdown of Aly and Uif potently blocks mRNA export, resulting in cell death in 6 days.

Here we provide evidence that Nxf1 inhibits its own RNA binding activity via an intramolecular interaction and that TREX components function to expose Nxf1's RNA binding domain, thereby allowing binding of the RNA to Nxf1. Thoc5 and Aly are essential for this process, and knockdown of these two proteins significantly reduces the amount of Nxf1 bound to mRNA *in vivo*. These results suggest that TREX is the major complex used to recruit Nxf1 to mRNA in human cells.

## Results

### TREX acts as a binding platform for Nxf1

To determine whether Nxf1 associates with an assembled TREX complex, we immunoprecipitated Nxf1 from a cell extract treated with RNase A to disrupt protein interactions bridged via mRNA (Supplementary Fig. S1). Following immunoprecipitation (IP), proteins were eluted under native conditions and identified by western blotting. This analysis revealed that multiple TREX components co-IP with Nxf1 (Fig. 1b). To determine whether these proteins were assembled in a single complex with Nxf1 or in multiple complexes, a secondary IP with Thoc5 antibody was carried out using the Nxf1 IP as starting material. Significantly, the secondary IP also contained Nxf1 and TREX components, indicating they can assemble into a single complex *in vivo*. We further established that Hpr1 binds Nxf1 (Fig. 1c) and this interaction is significantly reduced when the UBA domain is removed, indicating that the UBA domain plays an important role in the interaction with Hpr1 as it does in yeast<sup>19</sup>. Thus, TREX components Aly, Thoc5 and Hpr1 make contact with Nxf1.

### Thoc5 and Aly disrupt an Nxf1 intramolecular interaction

The Nxf1 domains are separated by flexible linkers<sup>21,22,7,23</sup> offering the possibility of conformational changes to Nxf1 on binding TREX. To examine this, we first carried out pull-down assays and found that GST-Nxf1:p15 interacts with full length Nxf1 and the isolated RBD and NTF2L domains (Fig. 2a, lanes 2-9). To investigate whether Nxf1:p15 might form an interdomain interaction between the RBD and NTF2L domains we carried out a pull-down assay with GST-NTF2L domain bound to p15 (Fig. 2a, lanes 10-12). Full length Nxf1 bound GST-NTF2L:p15 as did the RBD. This indicates that the NTF2L domain forms an interdomain interaction with the RBD. The LRR,  $\psi$ RRM and UBA domains did not show any binding activity in these experiments. Therefore, we cannot exclude the

possibility that these domains were non-functional or only partially functional. However, the UBA domain did bind a NUP214 fragment, indicating it retains some activity (Supplementary Fig. S2). As a further control, we confirmed that the RBD used in these studies retained RNA crosslinking activity, moreover this activity is conserved within amino acids 1-112 of *Drosophila melanogaster* Nxf1 (Fig. 2b), which also contains an arginine-rich region (Fig. 2c).

We confirmed that the RBD:NTF2L:p15 interaction was direct and reversible using pulldown assays with domains purified from *E.coli* (Fig. 2d). Binding of GST-NTF2L:p15 to GB1-RBD-6His was direct (Fig. 2d, lanes 8-10), and specific since it was reversed by additions of the purified competitor NTF2L:p15 (Fig. 2d lanes 11, 12). In Fig. 2d lane 7, a GB1-6His control construct was used in a pulldown with GST-NTF2L:p15 at a molar ratio 1:9 (GB1-6His/GST-NTF2L:p15), washed, and subsequently the competitor NTF2L:p15 was added at a molar ratio 1:9 (GB1-6His/NTF2L:p15). No GST-NTF2L:p15 or NTF2L:p15 are seen following pulldown indicating that these proteins do not bind non-specifically to either GB1-6His or the beads. Since the purified GB1-RBD-6His fragment of Nxf1 used in these assays has some visible minor truncations we cannot exclude the possibility that these also contribute to the binding of GST-NTF2L:p15 (Fig. 2d, lanes 8-10) or NTF2L:p15 (Fig. 2d, lanes 11,12).

To define the surface of the NTF2L domain bound by the RBD, we examined the interaction using a mutant NTF2L domain (456KHTR459 changed to 456AAAA459) which no longer binds Thoc5<sup>18</sup>. These mutations lie on the opposite face of the NTF2L domain to that which binds p15 (Fig. 3a,b) and do not alter the interaction with p15 (Fig. 3c and <sup>18</sup>). Surprisingly, we found that these NTF2L domain mutations enhance the interaction with the RBD (Fig. 3c). To define further residues required for the RBD:NTF2L interaction we generated additional mutations in the NTF2L domain. These mutations did not prevent p15 or a NUP214 fragment from binding the NTF2L domain, suggesting the overall fold of the domain is not perturbed (Supplementary Fig. S2). The R453D and the double mutant K456D-R459D significantly reduced the GST-RBD:NTF2L interaction (Fig. 3d). These residues cluster on the same surface that binds Thoc5 and opposite the face that binds p15 (Fig. 3b). Consistent with this, p15 is not required for the interaction between GST-RBD and the NTF2L domain (Fig. 3d, lane 2). The ability of the NTF2L R453D and K456D-R459D mutations to reduce the NTF2L:RBD association, together with the ability of the 456AAAA459 mutations to enhance binding, indicates this surface of the NTF2L domain is responsible for specific binding to the RBD.

Normally, it would be expected that intramolecular interactions between the NTF2L domain and the RBD would prevail over intermolecular interactions, yet the pulldown assay with Nxf1 and fragments does not distinguish these possibilities and only confirm that an interdomain interaction can occur. Thus, we examined Nxf1:p15 migration by gel filtration (Supplementary Fig. S3) and found that the majority of Nxf1:p15 behaves as a heterodimer (one molecule of Nxf1 complexed with 1 molecule of p15). Therefore, the intramolecular interaction predominates, though this experiment does not establish the proportion of the NTF2L and RBD domains bound to each other in free Nxf1. It was previously suggested that Nxf1 forms oligomers<sup>24</sup>, based on gel filtration of Nxf1 generated in reticulocyte lysate, though the high apparent molecular weight observed for Nxf1 in these earlier experiments could be explained by its association with other protein complexes in reticulocyte lysate.

Thoc5 and Aly bind the two Nxf1 domains implicated in the Nxf1 interdomain interaction. Therefore, we investigated whether they might influence this interaction. GST-Nxf1:p15 pulls down <sup>35</sup>S-Nxf1 (Fig. 4), and the addition of Aly or Thoc5 alone does not prevent this interaction. However, their combined presence does. Moreover, in the presence of Aly, more

Thoc5 associates with Nxf1, as reported previously<sup>18</sup>. Together, these data suggest that Thoc5 and Aly binding can disrupt the closed conformation of Nxf1.

### Nxf1 RNA binding is regulated by an intramolecular interaction

As the Nxf1 interdomain interaction involves its RBD, we investigated what impact this interaction has on Nxf1 RNA binding activity. Using UV cross-linking with purified proteins and 5' radiolabelled 15-mer RNA, we found that amino acids 1-372 of Nxf1, including the RBD, but lacking the inhibitory NTF2L domain, crosslinks with RNA more efficiently than full length Nxf1 (Fig. 5a). Moreover, when an Nxf1 fragment containing the RBD is affinity purified using the NTF2L domain fused to GST, and is therefore fully saturated with NTF2L domain, it fails to crosslink with RNA (Fig. 5b, lanes 6,7) whereas the free Nxf1 fragment containing the RBD binds RNA efficiently (Fig. 5b, lanes 1-5). In these experiments we used a GST pulldown as a control (Fig. 5b, lanes 10, 11) to confirm that the RBD is specifically binding GST-NTF2L rather than non-specifically precipitating with glutathione sepharose. Together, these data indicate that the Nxf1 interdomain interaction inhibits Nxf1's RNA binding activity. However, given that free Nxf1 is able to crosslink with RNA weakly, at steady state a proportion of Nxf1 is in an open conformation. Significantly, the NTF2L domain mutations, Nxf1 (456-459AAAA), which enhance the Nxf1 interdomain interaction, also reduce the ability of full length Nxf1 to cross-link with RNA *in vitro* (Fig. 5c). Since the *in vitro* RNA binding studies were carried out with an RNA oligonucleotide (Fig. 5a-c), we cannot exclude the possibility that the interaction of Nxf1 with mRNA *in vivo* might differ in its behaviour. However, Nxf1 (456-459 AAAA) also reduced the association of Nxf1 with the mRNP *in vivo* (Fig. 5d). Similarly, a mutant form of Nxf1, which harbors 10 arginine to alanine mutations in the RBD (10RA) and fails to bind the RNA used in these studies<sup>6</sup>, also fails to associate with poly(A)<sup>+</sup> RNA *in vivo* (Fig. 5d and <sup>6</sup>). Therefore, the Nxf1 (456-459 AAAA) mutations impaired Nxf1 RNA binding activity both *in vitro* and *in vivo*. To further examine the effects of the Nxf1(456-459AAAA) mutations on mRNA export, we used an RNAi complementation assay<sup>6</sup>. A wild type Nxf1 cDNA, resistant to RNAi efficiently complements an Nxf1 knockdown and restores normal mRNA export. However, the RBD mutant Nxf1(10RA)<sup>6</sup> or the Nxf1(456-459AAAA) mutations, both of which fail to bind RNA efficiently *in vitro* and *in vivo*, fail to complement Nxf1 RNAi, resulting in a robust nuclear accumulation of poly(A)<sup>+</sup> RNA in these cells (Fig. 5e). Together, these data indicate that Nxf1 RNA binding activity is regulated by its interdomain interaction.

### Thoc5 and Aly stimulate Nxf1 RNA binding

To establish whether Thoc5 and Aly, regulate Nxf1 RNA binding we carried out UV cross-linking assays. Both Thoc5 and Aly crosslink with RNA *in vitro*, although Thoc5 crosslinks less efficiently than Aly (Fig. 6a, lanes 1-6). Nxf1 also crosslinks weakly with RNA. However, in the presence of Thoc5 alone, the crosslink on Nxf1 is lost (Fig. 6a, lane 10). In the absence of Aly, Nxf1 remains a poor RNA crosslinker<sup>6</sup> and it is likely that the radiolabelled RNA, sequestered by the unbound Thoc5, was washed away prior to elution of the protein:RNA complex and UV crosslinking (Methods). Nevertheless, this result shows that Thoc5 alone does not enhance the RNA binding activity of Nxf1. In complex with Nxf1:p15, Aly stimulates Nxf1 RNA binding (Fig. 6a, lane 12), as reported previously<sup>6</sup>. The combination of Aly and Thoc5 further stimulates Nxf1's binding to RNA (Fig. 6a, lane 14), indicating both proteins are required for optimal Nxf1:RNA interactions. To investigate the contribution of Aly and Thoc5 to Nxf1:mRNA interactions *in vivo* we used an mRNP capture assay. Stable knockdown of either Aly or Thoc5 (Supplementary Fig. S4) did not prevent the Nxf1:mRNA interaction (Fig. 6b). However, double knockdown of Aly and Thoc5 led to a dramatic reduction in the amount of Nxf1 bound to mRNA *in vivo* (Fig. 6b), consistent with the ability of these proteins to disrupt the Nxf1 intramolecular interaction

and expose its RNA binding domain. In contrast, the interaction of Uap56 with mRNA, was not affected by Thoc5 and Aly RNAi (Fig. 6b), consistent with Uap56 functioning upstream of these TREX components in the mRNA export pathway<sup>20,25</sup>. We further investigated the effects of Aly and Thoc5 knockdown on mRNA export and found that, as reported previously<sup>18,20</sup>, single knockdown of Aly or Thoc5 had a modest impact on mRNA export (Fig. 6c), consistent with Nxf1's ability to bind mRNA under these conditions (Fig. 6b). In contrast, the Aly + Thoc5 combined knockdown caused a rapid and extreme mRNA export block (Fig. 6c), which led to cell death after 5 days. Since Thoc5 RNAi has a minimal impact on bulk mRNA export (Fig. 6c and <sup>18</sup>), these results rule out the possibility that the Nxf1(456-459AAAA) construct fails to complement Nxf1 RNAi (Fig. 5e) because it cannot bind Thoc5.

During mRNA export, Nxf1 associates with the FG repeats of nucleoporins at the nuclear pore and this can be detected by immunofluorescence in cells treated with Triton X-100 (TX) which allows release of the intranuclear Nxf1<sup>26</sup>. Since TREX components are required for the stable association of Nxf1 with the mRNP, we investigated whether they might also be required for the subsequent association of Nxf1 with the nuclear pore. In the absence of TX, Nxf1 shows a diffuse nuclear staining following a control RNAi treatment (Fig. 6d and Supplementary Fig. S5), whereas when cells are treated with TX, the diffuse intranuclear staining is reduced and the nuclear rim staining becomes prominent. This is also apparent when the fluorescence intensity across the nucleus is monitored, with clear peaks of Nxf1 staining at the nuclear rim (Fig. 6d, graphs on the right hand side). Following either Thoc5 or Aly RNAi, the nuclear rim staining for Nxf1 is still visible. In contrast, combined RNAi of Aly + Thoc5 dramatically reduced the nuclear rim association of Nxf1 and peaks of nuclear rim staining are not visible (Fig. 6d, graph right hand side and Supplementary Fig. S5). Interestingly, the intranuclear staining for Nxf1 in the presence or absence of TX was also increased following Aly + Thoc5 RNAi. To confirm that TX efficiently released soluble proteins from the 293 cell nucleus, we monitored the GFP signal produced by these stable RNAi cell lines and found consistently that TX treatment released GFP from these cells (Supplementary Fig. S6). These data indicate that Aly and Thoc5 are required for the Nxf1 nuclear rim association and in their absence Nxf1 appears trapped in a TX release-resistant state.

To further assess a requirement of TREX in allowing the recruitment of Nxf1 to the nuclear pores, we performed the TX release assay on cells stably knocked-down for both Aly and the largest THO-TREX subunit Thoc2. The combination of Aly and Thoc2 RNAi reduced the nuclear rim staining for Nxf1 (Fig. 7a). Moreover, whereas Aly RNAi led to a modest mRNA export block, the combined RNAi of Aly and Thoc2 led to a potent mRNA export block, as severe as that seen following Nxf1 RNAi (Fig. 7b). Following Nxf1 RNAi, there is a concomitant increase in the levels of Thoc2 in cells (Fig. 7c). Such compensatory increases in mRNA export factors following RNAi of other export factors have been reported previously<sup>2,20</sup> and underscore the important functional relationship between TREX and Nxf1.

## Discussion

Our data lead to a model in which Nxf1 sequesters its N-terminal RBD, through an intramolecular interaction with its NTF2L domain. In this model (Fig. 8), TREX binds to Nxf1, driving it into an open conformation, allowing it to stably bind mRNA and enable its export. Earlier studies have shown that RNAi of THO subunits leads to inhibition of mRNA export for a limited number of transcripts, including heatshock mRNAs<sup>9,18</sup>. In fact, depletion of Thoc5 in mouse cells only leads to a significant mRNA export block for ~2.9 % of mRNAs<sup>27</sup>. Similarly, loss of Aly does not cause a strong mRNA export block<sup>18, 20</sup>. We

also find that loss of Thoc5 or Aly alone does not prevent the association of Nxf1 with mRNA *in vivo* (Fig. 6), yet Nxf1 clearly binds an assembled TREX complex *in vivo* containing Aly and THO components (Fig. 1). The failure to detect a strong export block in the absence of Aly may be due to Uif which fulfils a similar role to Aly and is significantly up-regulated in the cell in response to Aly RNAi<sup>20</sup>. Likewise, the ability of the cell to maintain recruitment of Nxf1 to mRNA in the absence of Thoc5 alone, may be due to functional substitution by two other mRNA export factors that bind the Nxf1 NTF2L domain, Rbm15 and Rbm15B<sup>28</sup>. Despite redundant backup pathways to partially rescue mRNA export in the absence of single TREX components, disabling the TREX complex through RNAi of both Thoc5 and Aly largely prevents Nxf1 binding mRNA, leading to a concomitant rapid and lethal mRNA export block. Similarly knockdown of another THO complex component Thoc2 in combination with Aly RNAi leads to an mRNA export block. Together these data demonstrate an important role for the conserved THO-TREX complex in human mRNA export, although the precise repertoire of mRNAs which use the Nxf1 pathway in human cells still remains to be determined.

The *Drosophila melanogaster* orthologue of Nxf1 also harbors an N-terminal arginine rich region which has RNA binding activity (Fig. 2b,c) together with a conserved NTF2L domain<sup>29</sup>. Therefore, the regulation of Nxf1 RNA binding activity may be conserved across metazoa. Whether the yeast counterpart of Nxf1, Mex67, utilises a similar mechanism to bind mRNA and how this is controlled remain unclear as the N-terminal 100 amino acids of Mex67 does not show RNA binding activity<sup>21</sup>. Furthermore, Mex67 NTF2L domain and the p15 orthologue, Mtr2, have extended positively charged loop sequences that interact with rRNA *in vitro* and allow Mex67 to participate in the nuclear export of the 60S ribosomal subunit<sup>30</sup>. These extended loop sequences are absent in Nxf1 and p15. Furthermore yeast does not have a clear orthologue of THOC5. Therefore, these differences together with the lack of an apparent N-terminal RNA binding domain may partly explain the ability of Nxf1:p15 to only partially complement a Mex67:Mtr2 knockout<sup>31</sup>.

There is a clear overlap between the RBD and Thoc5 binding sites on the NTF2L domain of Nxf1 (Fig. 3) yet only the combination of Thoc5 and Aly can unlock Nxf1 (Fig. 4). Consistent with this observation, the weak binding of Thoc5 to Nxf1 *in vitro* is stimulated by Aly (Fig. 4 and 18). This suggests a two-stage mechanism for regulation of Nxf1 RNA binding whereby Aly partially destabilises the RBD interaction with the NTF2L domain, and this in turn facilitates Thoc5 binding and full displacement of the RBD from the NTF2L domain. As a consequence, maximal stimulation of Nxf1's RNA binding activity is achieved. It is striking that the RBD:NTF2L domain interaction involves a cluster of NTF2L domain positively charged residues (R453, K456 and R459) (Fig. 3), because Aly and SR proteins use a cluster of arginines to bind Nxf1<sup>32,33,6</sup>. Such arginine-rich peptides from Aly or SR proteins may compete with R453, K456 and R459 from the NTF2L domain for interaction with the Nxf1 RBD, thus triggering its partial displacement from the NTF2L domain. Although the Nxf1 RBD has no predicted secondary structure, a recent report suggests that this domain self-associates<sup>24</sup>. Therefore, Aly may also cause local rearrangement of the RBD, although we have not observed disruption of the RBD self-association in the presence of Aly. Instead, the folding of the RBD into a tertiary structure may be a prerequisite for its interaction with the NTF2L domain and subsequent interaction with mRNA.

Following combined knockdown of Aly and Thoc5, Nxf1 is no longer stably recruited to the mRNP. Furthermore, its nuclear rim association is reduced and a concomitant mRNA export block is observed. This implies that Nxf1 must be recruited to the mRNP to allow its subsequent docking at the nuclear pore and mRNA export. This may be because, upon recruitment to the mRNP, Nxf1 associates with proteins such as GANP which promote its

nuclear pore association<sup>34</sup>. When Nxf1 recruitment to the mRNP is disrupted, it accumulates in the nucleus in a TX insoluble fraction. We speculate that in this situation, Nxf1 becomes trapped with chromatin following its recruitment to transcription complexes via Hpr1 or other proteins and fails to be transferred to the mRNP via an assembled TREX complex.

The constitutive transport element of simple retroviruses binds Nxf1 with high affinity<sup>35</sup> and Nxf1 binds its own pre-mRNA, via a CTE-like structure within intron 10<sup>36</sup>. In each case, the interaction involves the  $\psi$ RRM and LRR domains<sup>37,22,21,38</sup>, which sit directly between the RBD and NTF2L domains. Therefore, it is conceivable that in order to bind Nxf1, the CTE has to disrupt the RBD:NTF2L interaction to gain access to the CTE binding site. Intriguingly, 9G8, which is capable of remodelling Nxf1 and allowing it to bind mRNA more efficiently<sup>6</sup>, stimulates CTE activity in a translation assay<sup>39</sup>. Therefore, 9G8 may stimulate opening of Nxf1, facilitating CTE:Nxf1 interactions. In the structure of a fragment of Nxf1 bound to the CTE<sup>38</sup>, the concave surface of the LRR and the alpha helical surface of the  $\psi$ RRM are exposed and do not make contact with the CTE. This leaves them available for interaction with proteins such as 9G8, which is known to bind the RBD- $\psi$ RRM fragment of Nxf1<sup>15</sup>. Furthermore, there is a pronounced kink between the  $\psi$ RRM and LRR domains of Nxf1 once bound to the CTE<sup>38</sup>, yet a significant proportion of the CTE is left solvent-exposed. The authors speculated that the NTF2L and UBA domains and p15 may also contribute to the interaction with the CTE, by encapsulating it, as may the N-terminal RBD. Such a CTE encapsulating conformation for Nxf1 may bring the RBD and NTF2L domains into close proximity, similar to the closed conformation we propose here for free Nxf1. Alternatively, the model of two Nxf1 molecules bound to a full length CTE<sup>38</sup> presents the Nxf1 molecules bound in a head to tail conformation on the CTE, which would potentially juxtapose the NTF2L and RBD domains from separate Nxf1 molecules, facilitating intermolecular NTF2L:RBD interactions and these may assist in establishing Nxf1:CTE interactions. Such a mode of Nxf1 binding the CTE would clearly diverge from the mechanism used by Nxf1 to bind cellular mRNA, yet suggests that the CTE might exploit the natural propensity of the Nxf1 RBD and NTF2L domains to interact for efficient binding.

If Nxf1 is directly tethered to an unspliced pre-mRNA via an MS2 coat protein and operator, the pre-mRNA is exported to the cytoplasm without undergoing splicing<sup>32</sup>. Therefore, it is vital for the cell to regulate Nxf1's RNA binding activity so that it only binds and exports processed mRNA. Our data indicate that Thoc5 and Aly regulate Nxf1 RNA binding activity, providing a molecular timer, which ensures that Nxf1 is only loaded onto mRNA once these two proteins have assembled within TREX. TREX assembly is coupled with splicing<sup>10</sup>, and the interaction of Aly with the 3' end processing factor Pcf11 indicates its recruitment to TREX might also be coupled with pre-mRNA 3' end processing<sup>14</sup>. We suggest that TREX assembly provides a mark on mRNA to signify that nuclear RNA processing events are complete and Nxf1 deciphers this mark and exports the processed mRNA to the cytoplasm. Of considerable interest now is to establish what other nuclear processes might make use of this molecular timer as recent reports suggest that siRNA production in plants also requires the TREX complex<sup>40, 41</sup>.

## Methods

### Reagents and cell lines

FLAG-Nxf1 and FLAG-Nxf1(10RA) contain the wild type and mutant Nxf1 cDNA respectively, subcloned into p3XFLAG-myc-CMV-26 expression vector (Sigma)<sup>6</sup>. GST-Nxf1:p15 comprises the Nxf1 cDNA subcloned in pGEX6P1(GE Healthcare) and this was cotransformed into *E.coli* BL21 RP strain with the p15 cDNA subcloned in pET9 (Novagen) for expression of the Nxf1:p15 heterodimer<sup>6</sup>. GB1-6His-Aly<sup>6</sup> contains ALYREF2 cDNA

subcloned into pET24b containing the GB1 solubility tag. FLAG-eGFP<sup>42</sup> contains the EGFP gene subcloned into p3XFLAG-myc-CMV-26 expression vector (Sigma). Mutations in Nxf1 were generated by Quikchange mutagenesis following the manufacturer's instructions (Stratagene). The Nxf1 cDNA encoding aa 1-550 (Nxf1 $\Delta$ UBA mutant) was amplified by PCR and cloned on an *NdeI/XhoI* fragment into pET24b-GB1<sup>20</sup>. The open reading frame of Thoc5 was cloned on an *NdeI/XhoI* fragment into pET24b. A cDNA fragment of the *Drosophila melanogaster* Nxf1 gene corresponding to amino acids 1-112 was amplified by reverse transcriptase-PCR using RNA isolated from fly strain W<sup>1118</sup> using the following oligonucleotides: 5' GAATTCATATGCCCAAACGCGGCGGTGGCAGTA and 5' GCGGATCTCGAGTTAGCCAAAGCTGTTGGGCATCAGTTTGCCG. The cDNA fragment was cloned on an *NdeI/XhoI* fragment into pET24b-GB1 as described in<sup>20</sup>. GB1-His tagged proteins were purified on TALON® resin following the manufacturer's instructions (Clontech). Human inducible FLP-In T-REX 293 RNAi cell lines were constructed as described previously<sup>20</sup> using the following target sequences: Aly #5 (CCGATATTCAGGAAGCTTTG), Thoc5 #1 (GGCAAGGATGTGGCAATAGAA), Thoc5 #2 (TTTGTTTCAGGCCACTGCGTAT), Thoc2 #1(AAGCATGAACAGGCATCTAAT), Thoc2 #3(TCTACAGAGATTGAAACTGGA), Nxf1 #1(GAACACGATGATGAACGCGTT), Nxf1 #3(GATGACATGTCTAGCATTGTT). Hairpins Thoc5 #1 and Thoc5 #2, Thoc2 #1 and Thoc2 #3, Nxf1 #1 and Nxf1 #3, were chained following the manufacturer's (Invitrogen) instructions by using *BglII* and *XhoI* sites and *BamHI/BglII* compatible ends. These combinations of hairpins were further chained with Aly hairpins using the same principle to generate Aly+Thoc5 or Aly+Thoc2 targeting constructs. miRNA expression was induced with 1  $\mu$ g/ml tetracycline (Sigma), concomitantly inducing the expression of EmGFP<sup>20</sup>. The Hpr1 and Nxf1 monoclonal antibodies were from Abcam and both used at 1:1000 for Western Blotting. Nxf1 antibody was also used at 1:500 for immunofluorescence. The anti-Aly, anti-FLAG, anti-Tubulin, and anti-6His monoclonals were from Sigma and used for western blotting at 1:20000, 1:5000, 1:5000, and 1:2000 respectively. A polyclonal antibody to Thoc5 was raised against 6His-Thoc5 (Supplementary Fig. S7) and used in western blotting at 1:2000 dilution. The Thoc2<sup>10</sup> and UAP56<sup>20</sup> antibodies were used at dilutions of 1:1000 and 1:2000 respectively. FLAG-agarose and FLAG peptide were from SIGMA.

### Sequential immunoprecipitations

10  $\times$  10 cm dishes of 293T cells were each transfected with either 18  $\mu$ g of FLAG-Nxf1 or FLAG-eGFP vectors. 48 hours after transfection, each dish was lysed in 1 ml of IP lysis buffer (50 mM HEPES pH 7.5, 100 mM NaCl, 1 mM EDTA, 1 mM DTT, 0.5 % Triton X-100, 10 % glycerol) + 10  $\mu$ g/mL RNase A). The cleared extracts were incubated with 150  $\mu$ L of  $\alpha$ -FLAG-agarose beads for one hour. The beads were then washed with 3  $\times$  5 mL of IP lysis buffer and the bound proteins were subsequently eluted in 1 mL of IP lysis buffer + FLAG peptide 100 ng/ $\mu$ L). 50  $\mu$ L of polyclonal  $\alpha$ -Thoc5 were bound to 30  $\mu$ L of Protein G-Sepharose. The eluate from the first IP was incubated with these  $\alpha$ -Thoc5-beads for one hour. The beads were then washed with 3  $\times$  900  $\mu$ L of IP lysis buffer. The bound proteins were finally eluted from the protein G-Sepharose with 70  $\mu$ L of [0.2 M glycine pH 2.8, 1 mM EDTA], and analysed by SDS-PAGE (10-12%) and Western Blot with the indicated antibodies.

### GST-pulldown experiments

For oligo(dT) pulldown assays the indicated GST-fusion constructs were expressed and purified using glutathione sepharose according to the manufacturer's instructions (GE Healthcare). The binding reactions were performed in 0.4-1 mL of either PBS-T buffer (1X Phosphate buffered saline (PBS), 0.1 % Tween) for Nxf1 domains interactions or RB100 buffer (25 mM HEPES pH 7.5, 100 mM KOAc, 10 mM MgCl<sub>2</sub>, 1 mM DTT, 0.05 % Triton

X-100, 10 % Glycerol) when Thoc5 or Aly were present and for figures 1c and 2d. Both buffers contained RNase A (10  $\mu\text{g}/\text{ml}$ ) and subsequent washes used the same buffers containing RNase A. The pulldown in Fig. 2d also contained 0.05% BSA as blocking agent and bound proteins were eluted from the IgG beads using 1% SDS at room temperature. For Fig. 5b, the pulldowns were performed in PBS-T buffer containing RNase A. The bound proteins were then washed first with PBS-T buffer, then RB100 buffer, and then eluted with 50 mM Tris HCl (pH 8.2), 40 mM GSH-reduced, 100 mM KOAc. The subsequent UV-crosslinking of the eluted [GST-NTF2L:p15 + 6His-RBD- $\psi$ RRM-LRR] complexes or of free 6His-RBD- $\psi$ RRM-LRR with radiolabeled RNA was performed in this elution buffer and as described below. For the GST-pulldown experiments presented in Fig. 1c, 1 ml of *E.coli* total cell extract (6 mg/ml) containing Nxf1:p15 or Nxf1 $\Delta$ UBA:p15 were used and proteins detected by Coomassie staining and Western blotting as indicated. For the NTF2L:p15 competitor used in the pulldown assay in Fig. 2d, GST-NTF2L:p15 was first purified on glutathione-coated beads (GE Healthcare) before on-bead cleavage with Prescission Protease. Cleaved and diluted NTF2L:p15 was desalted on G25 (GE Healthcare) in 20 mM Tris pH8.0, 25 mM NaCl before further purification on a 1 ml Mono-Q column (GE Healthcare). Resulting NTF2L:p15 was dialysed against RB100 buffer.

For transfection-based assays, one 6-cm dish of 293T cells per condition was used and was transfected with 6  $\mu\text{g}$  of the desired FLAG construct for 48 hours. For assays involving endogenous proteins, one 15-cm dish per cell line or condition was used. Cells were UV-crosslinked in PBS with 300  $\text{mJ}/\text{cm}^2$  and then lysed in the IP lysis buffer described above. The extracts were cleared by centrifugation at 16100  $\times$  g for 5 min. 1 mg (for transfection-based assays) or 2 mg (for endogeneous proteins assays) of total proteins were denatured in Binding Buffer (10 mM Tris HCl pH 7.5, 0.5 M NaCl, 0.5 % SDS, 0.1 mM EDTA) then incubated with 25  $\mu\text{L}$  (bed volume) of oligo(dT)-cellulose beads (Sigma) for one hour at room temperature. The beads were then washed with 3  $\times$  900  $\mu\text{L}$  of Binding Buffer. The mRNPs were finally eluted for 30 min in [10 mM Tris HCl pH 7.5, 1 mM EDTA, 50  $\mu\text{g}/\text{mL}$  RNase A], analysed by SDS-PAGE and Western Blotting with the indicated antibodies.

### UV-crosslinking experiments

A 5'-radiolabeled 15-mer RNA (5'-CAGUCGCAUAGUGCA-3') described previously<sup>42</sup> was incubated with the indicated proteins for 15 min on ice in 20  $\mu\text{L}$  of RNA binding buffer (15 mM HEPES pH 7.9, 0.2 mM EDTA, 5 mM  $\text{MgCl}_2$ , 0.05 % Tween-20, 10 % Glycerol, 100 mM NaCl). The reactions were then UV-irradiated for 10-15 min on ice and then analysed by SDS-PAGE. The gels were dried and the results were visualized by phosphorimaging. The UV-crosslinking experiment from Fig. 4a was done essentially as described previously<sup>6</sup>. 9 ng of 15-mer RNA were incubated for 10 min at room temperature with 50  $\mu\text{g}$  of Aly alone or 5  $\mu\text{g}$  of Thoc5 alone, or a combination of both Aly and Thoc5 before adding 2.5  $\mu\text{g}$  of immobilized GST-Nxf1:p15. After pulldown, the beads were washed to remove unbound RNA and proteins, and eluted complexes were UV-irradiated on ice. Complexes were analyzed by SDS-PAGE, stained with Coomassie blue and PhosphorImaging.

### Fluorescence *in situ* hybridization

Cells grown on coverslips were fixed at room temperature for 30 minutes with 11.1% paraformaldehyde in PBS. Cells were washed in PBS then incubated for 2 hours at 37  $^{\circ}\text{C}$  with hybridisation solution (20% formamide, 2  $\times$  sodium saline citrate (SSC), 10% dextran sulphate and 1% BSA) containing 1  $\text{ng}/\mu\text{l}$  Cy3 labelled oligo (dT)<sub>50</sub>, 0.5  $\mu\text{g}/\mu\text{l}$  single stranded DNA and 0.5  $\mu\text{g}/\mu\text{l}$  tRNA and subsequently washed 3 times sing PBS before mounting on glass slides for microscopy analysis.

## Immunostaining

Stable 293 cell lines were fixed in paraformaldehyde and permeabilized with Triton X-100 72 hours after induction of the expression of miRNAs targeting the specified genes. When indicated (+ TX), the cells were treated with 0.5% of Triton X-100 for one minute on ice prior to fixation and immunostaining. The fluorescence intensity scans were performed on the indicated cells using the ImageJ software (NIH) with a line width of 10 and a length of 100.

## Supplementary Material

Refer to Web version on PubMed Central for supplementary material.

## Acknowledgments

We thank Vicky Porteous for technical support and Nina Bausek for providing *D.melanogaster* RNA. SW acknowledges support from the BBSRC, Wellcome Trust and P.A. Banner Cancer Research Fund. RR and EF acknowledge support from NIH (GM043375).

## References

1. Herold A, Klymenko T, Izaurralde E. NXF1/p15 heterodimers are essential for mRNA nuclear export in *Drosophila*. *RNA*. 2001; 7:1768–1780. [PubMed: 11780633]
2. Herold A, Teixeira L, Izaurralde E. Genome-wide analysis of nuclear mRNA export pathways in *Drosophila*. *Embo J*. 2003; 22:2472–2483. [PubMed: 12743041]
3. Rodriguez-Navarro S, Hurt E. Linking gene regulation to mRNA production and export. *Curr Opin Cell Biol*. 2011; 23:302–309. [PubMed: 21227675]
4. Segref A, et al. Mex67p, a novel factor for nuclear mRNA export, binds to both poly(A)+ RNA and nuclear pores. *Embo J*. 1997; 16:3256–3271. [PubMed: 9214641]
5. Zolotukhin AS, Tan W, Bear J, Smulevitch S, Felber BK. U2AF participates in the binding of TAP (NXF1) to mRNA. *J Biol Chem*. 2002; 277:3935–3942. [PubMed: 11724776]
6. Hautbergue GM, Hung ML, Golovanov AP, Lian LY, Wilson SA. Mutually exclusive interactions drive handover of mRNA from export adaptors to TAP. *Proc Natl Acad Sci U S A*. 2008; 105:5154–5159. [PubMed: 18364396]
7. Fribourg S, Braun IC, Izaurralde E, Conti E. Structural basis for the recognition of a nucleoporin FG repeat by the NTF2-like domain of the TAP/p15 mRNA nuclear export factor. *Mol Cell*. 2001; 8:645–656. [PubMed: 11583626]
8. Strasser K, et al. TREX is a conserved complex coupling transcription with messenger RNA export. *Nature*. 2002; 417:304–308. [PubMed: 11979277]
9. Rehwinkel J, et al. Genome-wide analysis of mRNAs regulated by the THO complex in *Drosophila melanogaster*. *Nat Struct Mol Biol*. 2004; 11:558–566. [PubMed: 15133499]
10. Masuda S, et al. Recruitment of the human TREX complex to mRNA during splicing. *Genes Dev*. 2005; 19:1512–1517. [PubMed: 15998806]
11. Jimeno S, Rondon AG, Luna R, Aguilera A. The yeast THO complex and mRNA export factors link RNA metabolism with transcription and genome instability. *Embo J*. 2002; 21:3526–3535. [PubMed: 12093753]
12. Dufu K, et al. ATP is required for interactions between UAP56 and two conserved mRNA export proteins, Aly and CIP29, to assemble the TREX complex. *Genes Dev*. 2010; 24:2043–2053. [PubMed: 20844015]
13. Cheng H, et al. Human mRNA export machinery recruited to the 5' end of mRNA. *Cell*. 2006; 127:1389–1400. [PubMed: 17190602]
14. Johnson SA, Cubberley G, Bentley DL. Cotranscriptional recruitment of the mRNA export factor Yra1 by direct interaction with the 3' end processing factor Pcf11. *Mol Cell*. 2009; 33:215–226. [PubMed: 19110458]

15. Huang Y, Gattoni R, Stevenin J, Steitz JA. SR splicing factors serve as adapter proteins for TAP-dependent mRNA export. *Mol. Cell.* 2003; 11:837–843. [PubMed: 12667464]
16. Strasser K, Hurt E. Yra1p, a conserved nuclear RNA-binding protein, interacts directly with Mex67p and is required for mRNA export. *Embo J.* 2000; 19:410–420. [PubMed: 10722314]
17. Golovanov AP, Hautbergue GM, Tintaru AM, Lian LY, Wilson SA. The solution structure of REF2-I reveals interdomain interactions and regions involved in binding mRNA export factors and RNA. *Rna.* 2006; 12:1933–1948. [PubMed: 17000901]
18. Katahira J, Inoue H, Hurt E, Yoneda Y. Adaptor Aly and co-adaptor Thoc5 function in the Tap-p15-mediated nuclear export of HSP70 mRNA. *Embo J.* 2009; 28:556–567. [PubMed: 19165146]
19. Gwizdek C, et al. Ubiquitin-associated domain of Mex67 synchronizes recruitment of the mRNA export machinery with transcription. *Proc Natl Acad Sci U S A.* 2006; 103:16376–16381. [PubMed: 17056718]
20. Hautbergue GM, et al. UIF, a New mRNA Export Adaptor Which Works Together with REF/ALY, Requires FACT for Recruitment to mRNA. *Curr Biol.* 2009; 19:1918–1924. [PubMed: 19836239]
21. Liker E, Fernandez E, Izaurralde E, Conti E. The structure of the mRNA export factor TAP reveals a cis arrangement of a non-canonical RNP domain and an LRR domain. *Embo J.* 2000; 19:5587–5598. [PubMed: 11060011]
22. Ho DN, Coburn GA, Kang Y, Cullen BR, Georgiadis MM. The crystal structure and mutational analysis of a novel RNA-binding domain found in the human Tap nuclear mRNA export factor. *Proc Natl Acad Sci U S A.* 2002; 99:1888–1893. [PubMed: 11854490]
23. Grant RP, Hurt E, Neuhaus D, Stewart M. Structure of the C-terminal FG-nucleoporin binding domain of Tap/NXF1. *Nat Struct Biol.* 2002; 9:247–251. [PubMed: 11875519]
24. Matzat LH, Berberoglu S, Levesque L. Formation of a Tap/NXF1 homotypic complex is mediated through the amino-terminal domain of Tap and enhances interaction with nucleoporins. *Mol Biol Cell.* 2008; 19:327–338. [PubMed: 17978099]
25. Luo ML, et al. Pre-mRNA splicing and mRNA export linked by direct interactions between UAP56 and Aly. *Nature.* 2001; 413:644–647. [PubMed: 11675789]
26. Bachi A, et al. The C-terminal domain of TAP interacts with the nuclear pore complex and promotes export of specific CTE-bearing RNA substrates. *RNA.* 2000; 6:136–158. [PubMed: 10668806]
27. Guria A, et al. Identification of mRNAs that are spliced but not exported to the cytoplasm in the absence of THOC5 in mouse embryo fibroblasts. *Rna.* 2011; 17:1048–1056. [PubMed: 21525145]
28. Uranishi H, et al. The RNA-binding motif protein 15B (RBM15B/OTT3) acts as cofactor of the nuclear export receptor NXF1. *J Biol Chem.* 2009; 284:26106–26116. [PubMed: 19586903]
29. Herold A, et al. TAP (NXF1) belongs to a multigene family of putative RNA export factors with a conserved modular architecture. *Mol Cell Biol.* 2000; 20:8996–9008. [PubMed: 11073998]
30. Yao W, et al. Nuclear export of ribosomal 60S subunits by the general mRNA export receptor Mex67-Mtr2. *Mol Cell.* 2007; 26:51–62. [PubMed: 17434126]
31. Katahira J, et al. The Mex67p-mediated nuclear mRNA export pathway is conserved from yeast to human. *Embo J.* 1999; 18:2593–2609. [PubMed: 10228171]
32. Hargous Y, et al. Molecular basis of RNA recognition and TAP binding by the SR proteins SRp20 and 9G8. *Embo J.* 2006; 25:5126–5137. [PubMed: 17036044]
33. Tintaru AM, et al. Structural and functional analysis of RNA and TAP binding to SF2/ASF. *EMBO Rep.* 2007; 8:756–762. [PubMed: 17668007]
34. Wickramasinghe VO, et al. mRNA export from mammalian cell nuclei is dependent on GANP. *Curr Biol.* 2010; 20:25–31. [PubMed: 20005110]
35. Gruter P, et al. TAP, the human homolog of Mex67p, mediates CTE-dependent RNA export from the nucleus. *Mol Cell.* 1998; 1:649–659. [PubMed: 9660949]
36. Li Y, et al. An intron with a constitutive transport element is retained in a Tap messenger RNA. *Nature.* 2006; 443:234–237. [PubMed: 16971948]

37. Braun IC, Rohrbach E, Schmitt C, Izaurralde E. TAP binds to the constitutive transport element (CTE) through a novel RNA-binding motif that is sufficient to promote CTE-dependent RNA export from the nucleus. *Embo J.* 1999; 18:1953–1965. [PubMed: 10202158]
38. Teplova M, Wohlbold L, Khin NW, Izaurralde E, Patel DJ. Structure-function studies of nucleocytoplasmic transport of retroviral genomic RNA by mRNA export factor TAP. *Nat Struct Mol Biol.* 2011; 18:990–998. [PubMed: 21822283]
39. Swartz JE, Bor YC, Misawa Y, Rekosh D, Hammarskjold ML. The shuttling SR protein 9G8 plays a role in translation of unspliced mRNA containing a constitutive transport element. *J Biol Chem.* 2007; 282:19844–19853. [PubMed: 17513303]
40. Yelina NE, et al. Putative Arabidopsis THO/TREX mRNA export complex is involved in transgene and endogenous siRNA biosynthesis. *Proc Natl Acad Sci U S A.* 2010; 107:13948–13953. [PubMed: 20634427]
41. Jauvion V, Elmayan T, Vaucheret H. The conserved RNA trafficking proteins HPR1 and TEX1 are involved in the production of endogenous and exogenous small interfering RNA in Arabidopsis. *Plant Cell.* 2010; 22:2697–2709. [PubMed: 20798330]
42. Hung ML, Hautbergue GM, Snijders AP, Dickman MJ, Wilson SA. Arginine methylation of REF/ALY promotes efficient handover of mRNA to TAP/NXF1. *Nucleic Acids Res.* 2010; 38:3351–3361. [PubMed: 20129943]

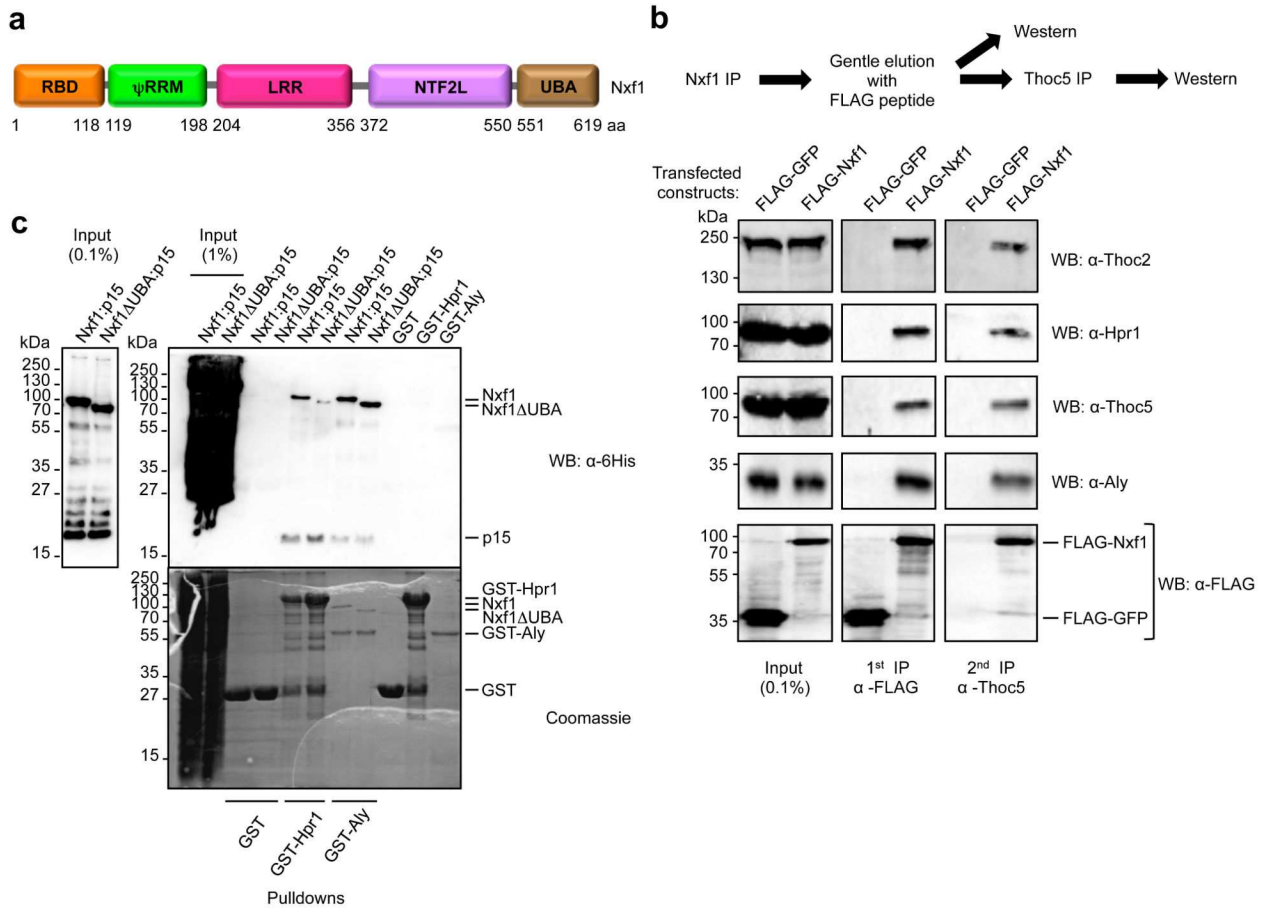


### Figure 1. Nxf1 and TREX assemble in a complex *in vivo*

(a) Schematic of Nxf1 showing its domains. RBD, RNA binding domain;  $\psi$ RRM, pseudo RNA recognition motif; LRR, leucine rich repeat; NTF2L, NTF2-like; UBA, ubiquitin associated. (b) Immunoprecipitation (IP) analysis of Nxf1. FLAG-Nxf1 was immunoprecipitated using FLAG antibody, eluted using FLAG peptide and then immunoprecipitated a second time using Thoc5 antibody. At each stage, samples were analysed by western blotting using the indicated antibodies. (c) The UBA domain of Nxf1 is required for interaction with Hpr1. GST-Hpr1 or GST-Aly pull-downs with the indicated Nxf1 constructs. Nxf1-GB1-6His or Nxf1 $\Delta$ UBA-GB1-6His were co-expressed with p15-6His in BL21RP *E. coli* strain. Total extracts were prepared, cleared by centrifugation, and used in pull-down experiments with GST-Hpr1 or GST-Aly in RB100 buffer in the presence of RNase A (10  $\mu$ g/mL). Pull-downs were analysed by SDS-PAGE followed by Coomassie staining or western blot using 6His antibody.



RBD was analysed by an IgG pulldown experiment performed in RB100 buffer in the presence of BSA (lane 1) and RNase A using purified GB1-6His or GB1-RBD-6His and GST-NTF2L:p15 (lanes 7-12). Unbound proteins were washed away and subsequently either buffer (lanes 8-10) or NTF2L:p15 competitor (lanes 7, 11, 12) was added at the indicated molar ratios. The GB1 tag binds IgG beads. Purified proteins used in this assay are shown in lanes 2-5. Bound proteins were eluted and subsequently analysed by SDS-PAGE and Coomassie staining. Lane 6 shows IgG binding and elution of GB1-RBD-6His alone, performed in the same conditions as the pulldown assays. Additional bands, not present in the GB1-RBD-6His input sample, arising from the IgG beads are marked on the right hand side of the gel by brackets.

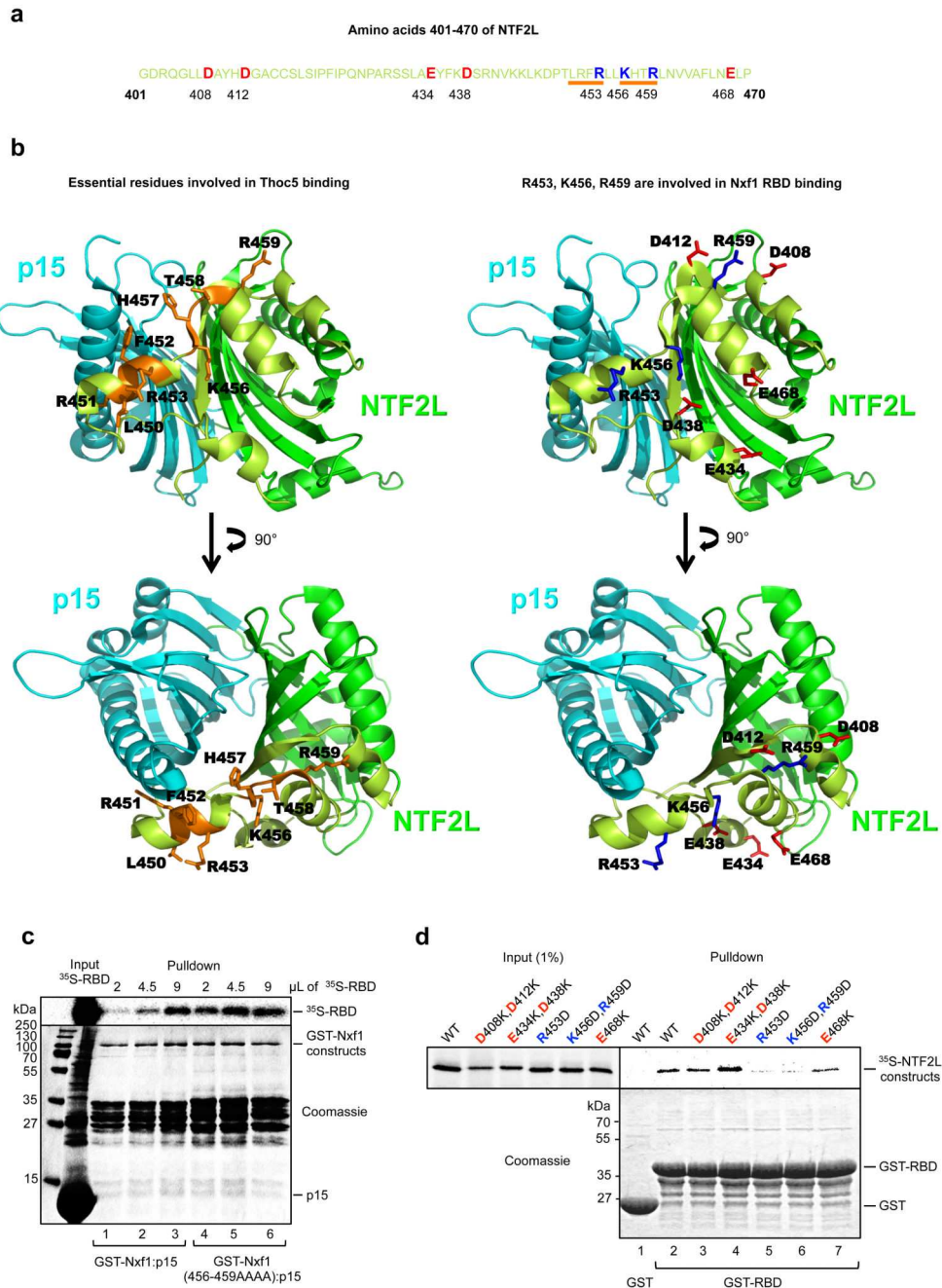


### Figure 3. Identification of the NTF2L:RBD binding interface

(a) Sequence of the region of the NTF2L domain targeted by the mutagenesis. Targeted residues are highlighted as red for acidic and blue for basic. Orange bars indicate the most crucial residues involved in Thoc5 binding (Katahira J. *et al*, EMBO J., 2009 Mar 4;28(5): 556-67) that also enhance Nxf1 interdomain interaction when mutated to alanines (in case of 456-459). (b) Positions of the above mentioned residues on NTF2L:p15 structure (1JKG) using the same colors as in (a). p15 is in cyan, the NTF2L domain is in dark green, targeted region within the NTF2L domain is in light green. (c) Nxf1(456-459AAAA) mutant binds Nxf1 RBD more efficiently than wild type Nxf1. GST pull-downs with the indicated fusions

and increasing amounts of  $^{35}\text{S}$ -RBD. (d) GST pulldown experiment using GST-RBD and the indicated *in vitro* translated mutants of the NTF2L domain of Nxf1.

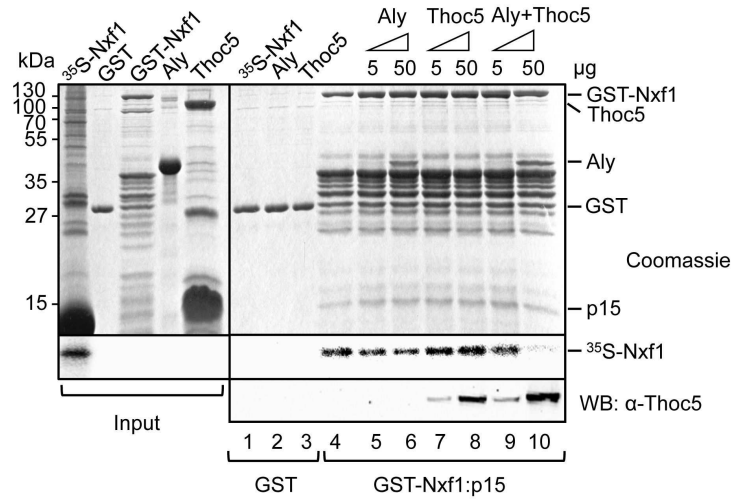


**Figure 4. Both Aly and Thoc5 are required to disrupt Nxf1-Nxf1 interactions**  
 Pull-down assays with GST-Nxf1:p15 and  $^{35}\text{S}$ -radiolabeled Nxf1 in the presence of the indicated TREX components. The lower panel is a Western blot to detect the binding of Thoc5. All of these experiments were carried out in the presence of RNase A.

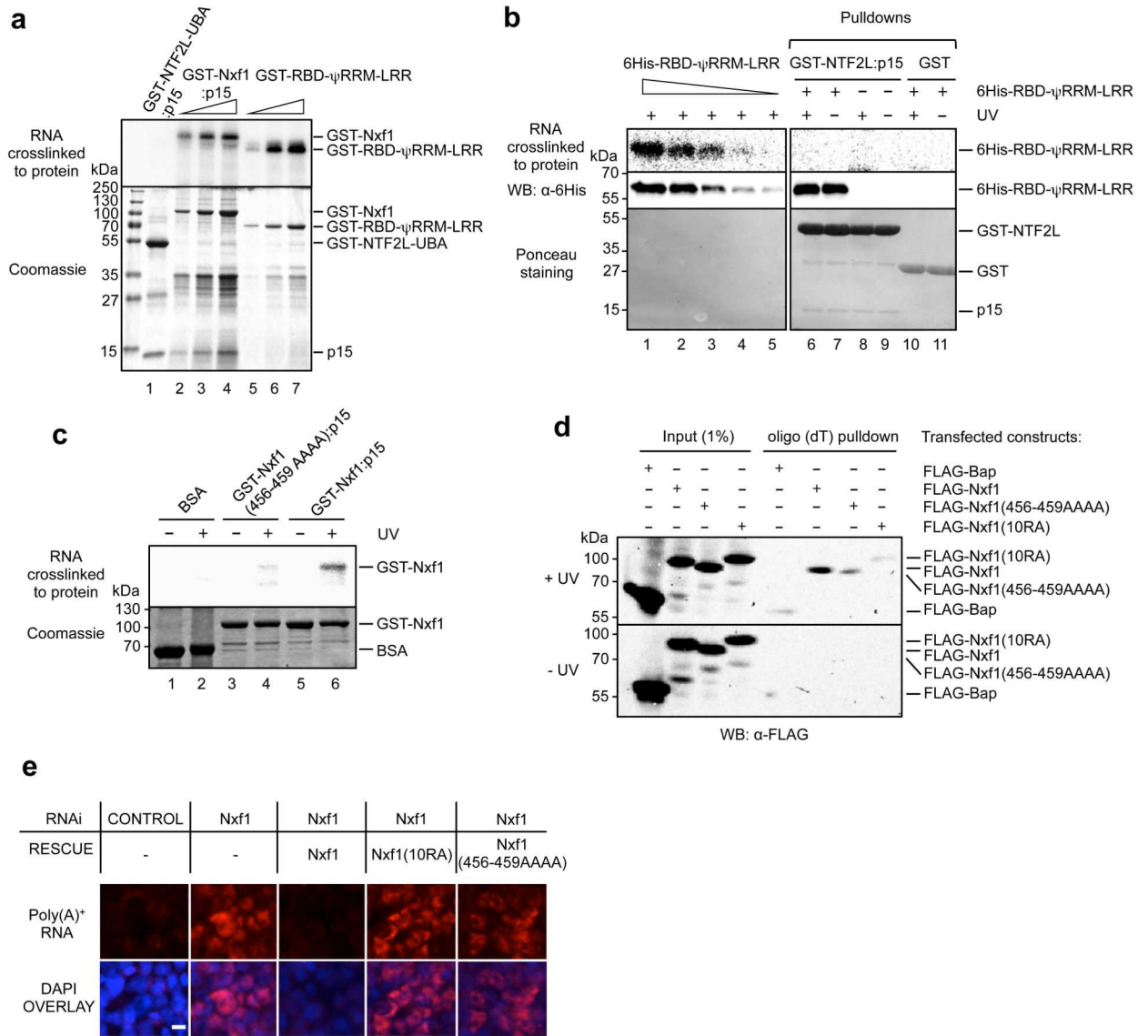


### Figure 5. The Nxf1 intramolecular interaction regulates its RNA binding activity

(a) RNA cross-linking activity for GST-TAP:p15 and GST-RBD- $\psi$ RRM-LRR. The three different Nxf1 construct protein concentrations used (from left to right) were 88, 265 and 530 nM and the RNA concentration was 6.5  $\mu$ M. (b) The Nxf1 RBD fails to bind RNA when complexed with the NTF2L domain. The 6His-RBD- $\psi$ RRM-LRR protein efficiently crosslinks with RNA (top panel lanes 1-5, using 200, 100, 50, 20, 10 ng of protein). RNA binding was detected by phosphoimaging. 6His-RBD- $\psi$ RRM-LRR was detected by Western blot (middle panel) and the GST constructs were detected by Ponceau staining (bottom panel). (c) RNA cross-linking activity for GST-Nxf1(456-459AAAA):p15 and GST-Nxf1:p15. RNA binding was detected by phosphoimaging. (d) mRNP capture assay with indicated Nxf1 constructs. Bap is bacterial alkaline phosphatase control. Nxf1(10RA) is a mutant form of Nxf1 which is unable to bind RNA efficiently<sup>6</sup>. (e) RNA export assay in 293T cells. Cells were transfected with the Nxf1 RNAi vector together with the indicated rescue Nxf1 expression vectors, resistant to RNAi. Cells were analysed by fluorescent *in situ* hybridisation (FISH) with Cy3-oligo(dT) (top panel) and images overlaid with DAPI

staining of the same cells (bottom panel). All pictures were taken at the same exposure level. The white horizontal bar represents 10  $\mu\text{m}$ .



TREX components Aly and Thoc5 are depleted by RNAi. After 72 hours of induction of miRNAs expression, the indicated 293 stable RNAi cell lines were subjected to Triton X-100 extraction prior to fixation when indicated (+ TX) and the localisation of Nxf1 was analysed by immunostaining  $\alpha$ -Nxf1 and fluorescence intensity scanning (white bars and corresponding graphs). The Y-axis of the graphs represents the pixel intensity (Px Int.) and the X-axis the distance in pixels (Dist. (px)). The white horizontal bars in (c) and (d) represent 10  $\mu$ m.

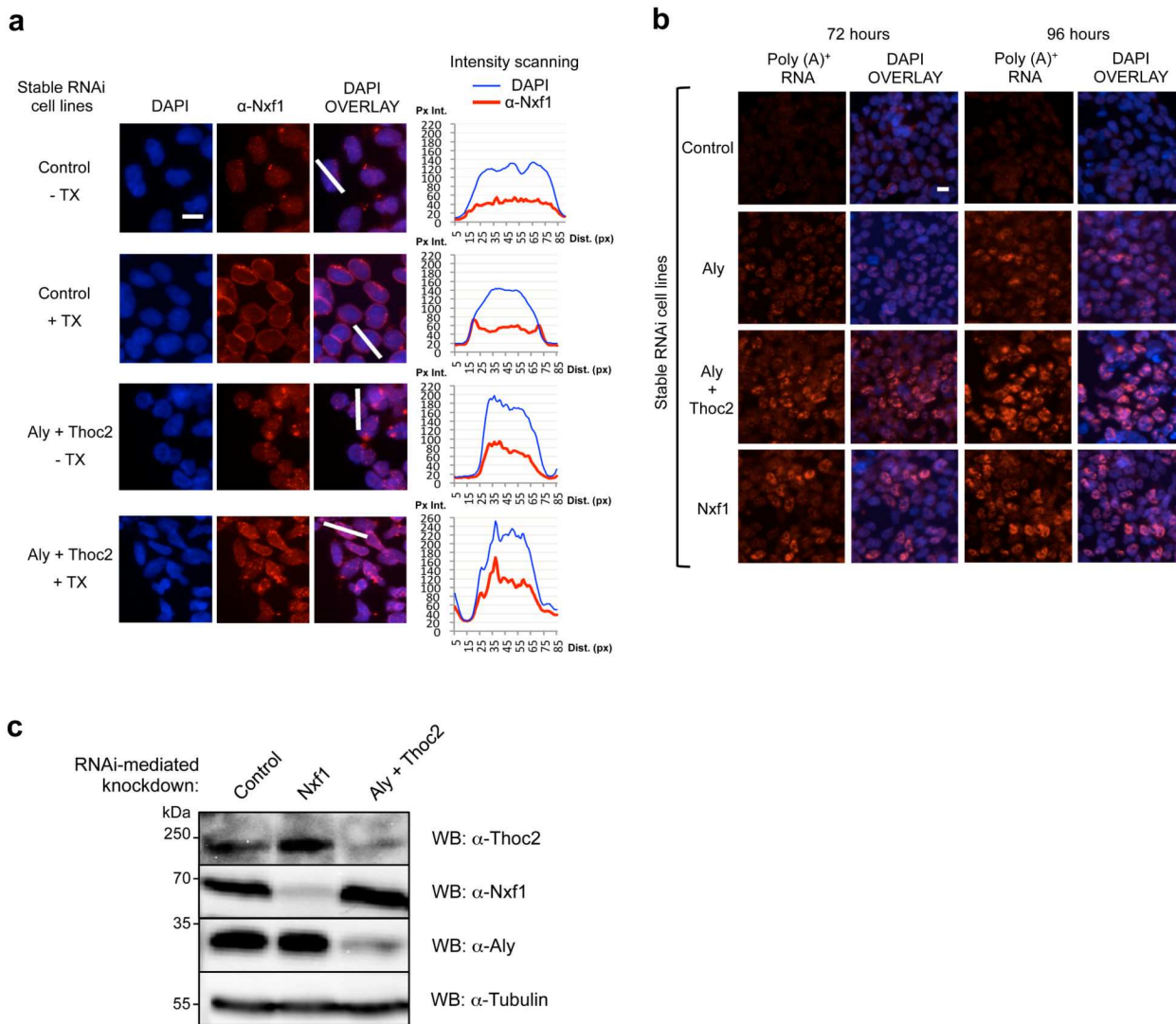


**Figure 7. Thoc2 plays a role in Nxf1 localisation and mRNA export**

(a) Nuclear envelope association of Nxf1 is impaired *in vivo* when both TREX components Aly and Thoc2 are depleted by RNAi. Localisation of Nxf1 was analysed by immunostaining of Control or (Aly+Thoc2) knockdown cell lines after 96h of induction of miRNA expression using Nxf1 antibody. Where indicated (+ TX), cells were treated with 0.5% Triton X-100 before fixing. The Y-axis of the graphs represents the pixel intensity (Px Int.) and the X-axis the distance in pixels (Dist. (px)). (b) A strong block of bulk poly(A)<sup>+</sup> RNA export is observed in Nxf1 RNAi and (Aly+Thoc2) RNAi cell lines. Oligo (dT) FISH on stable 293 cell lines expressing miRNAs targeting the indicated genes. The time points refer to the time following induction of miRNAs expression. Cells were treated with actinomycin D for 2 hours prior to FISH to reduce nascent RNA signals. All pictures are taken at the same exposure level. The white horizontal bars in (a) and (b) represent 10 μm. (c) Western Blot analysis of the indicated cell lines. The expression of the miRNAs is under the control of a tetracycline inducible promoter. Extracts were prepared 96 hours post-induction of miRNA expression and analysed using the indicated antibodies.

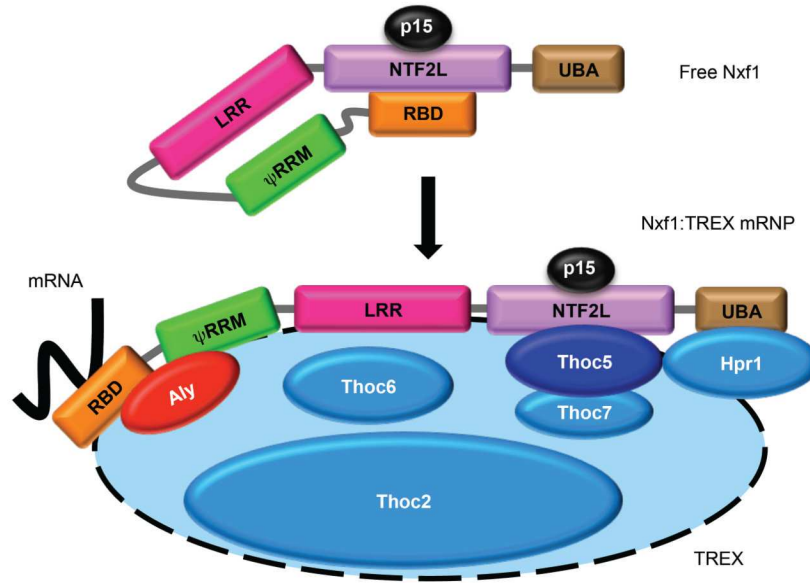


**Figure 8. A model for the conformational change in Nxf1 induced by TREX during mRNA export**

Free Nxf1:p15 sequesters its N-terminal RNA binding domain. During mRNA export, assembled TREX binds Nxf1:p15. This allows the two subunits Aly and Thoc5 to remodel Nxf1 and expose its RNA binding domain, allowing direct interaction between Nxf1 and mRNA during export. For clarity not all TREX subunits are illustrated in the figure.